AJNR

Temporomandibular Joint: MR Imaging of Internal Derangements and Postoperative Changes

Kurt P. Schellhas, Clyde H. Wilkes, Hollis M. Fritts, Mark R. Omlie, Kenneth B. Heithoff and Jeffrey A. Jahn

AJNR Am J Neuroradiol 1987, 8 (6) 1093-1101
http://www.ajnr.org/content/8/6/1093

Temporomandibular Joint: MR Imaging of Internal Derangements and Postoperative Changes

Kurt P. Schellhas[1]
Clyde H. Wilkes[2]
Hollis M. Fritts[1]
Mark R. Omlie[3]
Kenneth B. Heithoff[1]
Jeffrey A. Jahn[1]

Nineteen abnormal temporomandibular joints (TMJs) imaged with high-field-strength surface-coil MR are presented to illustrate specific changes associated with disk derangement, trauma, and previous surgery. Cases were selected from a series of 248 TMJ MR studies in 144 patients (9–68 years old, 130 females and 14 males) performed during a 5-month period. Surgical findings were available for correlation in 44 of the 248 joints studied. Increased signal caused by myxoid degeneration within the degenerating meniscus was seen, as were pathologic changes including atrophy, fibrosis, and contracture of masticatory muscles occurring with internal degrangements. Advantages and limitations of MR are discussed with reference to arthrography and videofluoroscopy. High-resolution and partial-flip-angle images of a normal joint are provided for comparison.

In most clinical circumstances, MR is the procedure of choice when examining the TMJ, because it provides contrast resolution of soft-tissue structures superior to that of conventional imaging techniques.

MR is an established technique for diagnosing internal derangements of the temporomandibular joint (TMJ) [1–5]. The lack of ionizing radiation and noninvasive characteristics of MR make it the examination of choice over arthrography in most clinical circumstances. MR provides superior contrast resolution of soft-tissue structures as compared with conventional imaging procedures. Our intention is to present TMJ alterations imaged with a 1.5-T magnet. We report changes observed with trauma and various surgical procedures and describe our early experience with partial-flip-angle imaging techniques.

Materials and Methods

Two hundred forty-eight TMJ MR studies were performed in 144 patients between January 2 and May 30, 1987, with a 1.5-T GE imaging system using an 8.9-cm surface coil. The first 56 joints in the series were imaged with T1-weighted 3-mm-thick contiguous interleaved partial-saturation images that had a repetition time (TR) of 500 msec, echo time (TE) of 20 msec, 256 × 128 matrix with four signal acquisitions, and 12-cm field of view for the closed-mouth series and two acquisitions for the open-mouth sequence. The last 192 joints in the series were studied with contiguous 3-mm-thick sagittal images that had TR = 500 msec, TE = 20 msec, 256 × 256 matrix, and two acquisitions for the closed-mouth series. Open-mouth views were obtained with 3-mm images with a 2-mm gap and two acquisitions. Closed- and open-mouth examinations required 8 min 35 sec and 4 min 18 sec, respectively. Selected cases were examined with the spin-echo technique (TR = 2000 msec, TE = 20/80 msec) if inflammatory disease or joint fluid was suspected. Occasionally, nine contiguous interleaved 3-mm-thick T1-weighted coronal images were obtained through the condyle and pterygoid muscles with TR = 500 msec, TE = 20 msec, 256 × 256 matrix, and one acquisition, mostly to assess suspected bony and muscular disease. Nine sagittal images were obtained through the full width of the condyles after obtaining a short axial localizing sequence (Fig. 1). Most patients (all cases reported) were screened with preliminary submentovertex and open-mouth, jaw-protruded anteroposterior radiographs of the skull base and closed- and open-

This article appears in the November/December 1987 issue of *AJNR* and the February 1988 issue of *AJR*.

Received March 2, 1987; accepted after revision June 22, 1987.

Presented at the annual meeting of the American Society of Head and Neck Radiology, Milwaukee, May 1987.

[1] Center for Diagnostic Imaging, 5775 Wayzata Blvd., Suite 190, St. Louis Park, MN 55416. Address reprint requests to K. P. Schellhas.

[2] Park Place Center, Suite 990, 5775 Wayzata Blvd., St. Louis Park, MN 55416.

[3] 250 Central Ave. N., Wayzata, MN 55391.

***AJNR* 8:1093–1101, November/December 1987**
0195–6108/87/0806–1093

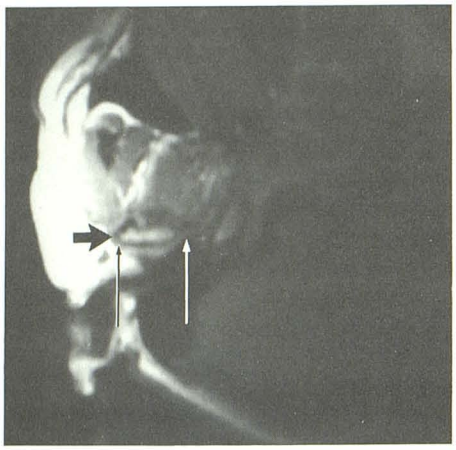

Fig. 1.—T1-weighted axial localizing image (TR = 400 msec, TE = 20 msec, one acquisition, 10 mm thick) prior to sagittal imaging. Patient and condyle (*thick arrow*) are rotated approximately 25° toward vertical surface coil to permit direct sagittal imaging perpendicular to condylar axis. Condylar orientation was predetermined with submentovertex skull radiograph. Imaging is performed from lateral pole of condyle to point beyond medial pole (*thin arrows*) to include lateral pterygoid muscles.

mouth lateral TMJ tomograms. The base view of the skull was used for head positioning relative to the surface coil in an attempt to obtain cephalometrically corrected sagittal MR images. Patients with restricted condylar translation were generally examined in the closed-mouth position only, particularly when significant meniscus displacement and intrinsic derangement was observed. Open-mouth views were obtained when only mild abnormalities were seen on closed-mouth images.

The last 52 joints (29 patients) in the series were studied routinely with a combination of standard T1-weighted closed-mouth and partial-flip-angle techniques or GRASS (gradient recalled acquisition in the steady state), which allowed for rapid sequential scanning of the joint in various stages of opening in as little as 3 sec per image. A technique with TR = 21 msec, TE = 12.5, and flip angle of 30° was used with a 128 × 256 matrix and 16.5-cm field of view. There was no change in patient positioning between standard and partial-flip-angle imaging sequences. A midcondyle location was selected for the single 5-mm-thick image that this technique yields with each imaging sequence. A Burnett TMJ device* was used to regulate the degree of mouth opening. Three to 12 sequential images with 3-mm opening steps were obtained for dynamic viewing of joints. Partial and fully open GRASS images were obtained in conjunction with the standard T1-weighted images in most cases. The average examination time for a bilateral closed-mouth-only examination was about 30 min, while bilateral closed- and open-mouth studies required an average of 50 min. Nine examinations were terminated because of claustrophobia. Six procedures were considered to be technically inadequate for diagnosis owing to patient motion. Nine examinations were inconclusive owing to limitations of spatial resolution and/or unusual anatomy. Arthrography and videofluoroscopy provided conclusive information in five of these nine inconclusive cases. Nine joints (nine patients) were also evaluated with dual-compartment arthrography and videofluoroscopy [6]. To date, surgical results are available in 44 joints from the series.

* Medrad, Inc., Pittsburgh.

Results and Discussion

Normal Joint Anatomy

Normal TMJ anatomy is sharply defined with surface-coil MR (Fig. 2) [2–8]. The normal meniscus is biconcave in appearance and is located between the articular surfaces of the mandibular condyle and temporal bone. The thickest portion of the posterior band of the meniscus is usually centrally situated on top of the condyle in coronal images. A normal meniscus emits a homogeneously low signal. Masticatory muscles and meniscal attachments are demarcated by adjacent fat (Figs. 2 and 3). The superior belly of the lateral pterygoid muscle attaches to the lateral pterygoid plate anteriorly and to the central and medial aspect of the anterior meniscus attachment posteriorly, and asserts traction on the normal meniscus during forward movement (translation) of the condyle. The inferior belly of the lateral pterygoid muscle extends between the inferior aspect of the lateral pterygoid plate and the fovea of the condylar neck and pulls the condyle forward during contraction. The medial pterygoid, the temporalis, and the masseter all function in jaw closure. Abnormalities of muscle function may be directly visualized with dynamic partial-flip-angle techniques [9].

It is important to note that standard T1-weighted open-mouth MR views frequently demonstrate a diminished amplitude of forward condylar translation owing to patient difficulty in maintaining a maximum open-mouth position for the time required for imaging, regardless of the presence or absence of internal derangement. This problem is completely solved with partial-flip-angle techniques, in which images are obtained in as little as 3 sec. T2* characteristics are accentuated with the partial-flip-angle technique used in the study.

Internal Derangements

Abnormalities of meniscus position and morphology are clearly defined with MR (Figs. 3–9). Most internal derangements involve soft-tissue structures, which may be impossible to demonstrate with noninvasive conventional imaging techniques. Anterior displacement of the meniscus is the most common internal derangement affecting the TMJ. With forward meniscus displacement, the posterior attachment (bilaminar zone) is stretched and may exhibit either attenuation or thickening and redundancy (Figs. 5 and 7). Medial or lateral displacement commonly accompanies anterior meniscus displacement and advanced internal derangements. Medial vs lateral meniscus displacement can be determined from sequential sagittal images alone if they cover the full width of the condyle; however, when there is unusual condylar anatomy, coronal images may be applied (Fig. 6). The combination of anterior and medial meniscus displacement is a frequent cause of clinical "closed lock." Thickening and deformity of the meniscus may be observed. Perforations of the meniscus and attachments may be diagnosed (Figs. 7 and 8). Perforation is a common false-positive finding with MR owing to the often attenuated appearance of the stretched bilaminar zone in cases of chronic anterior displacement. Abnormalities of

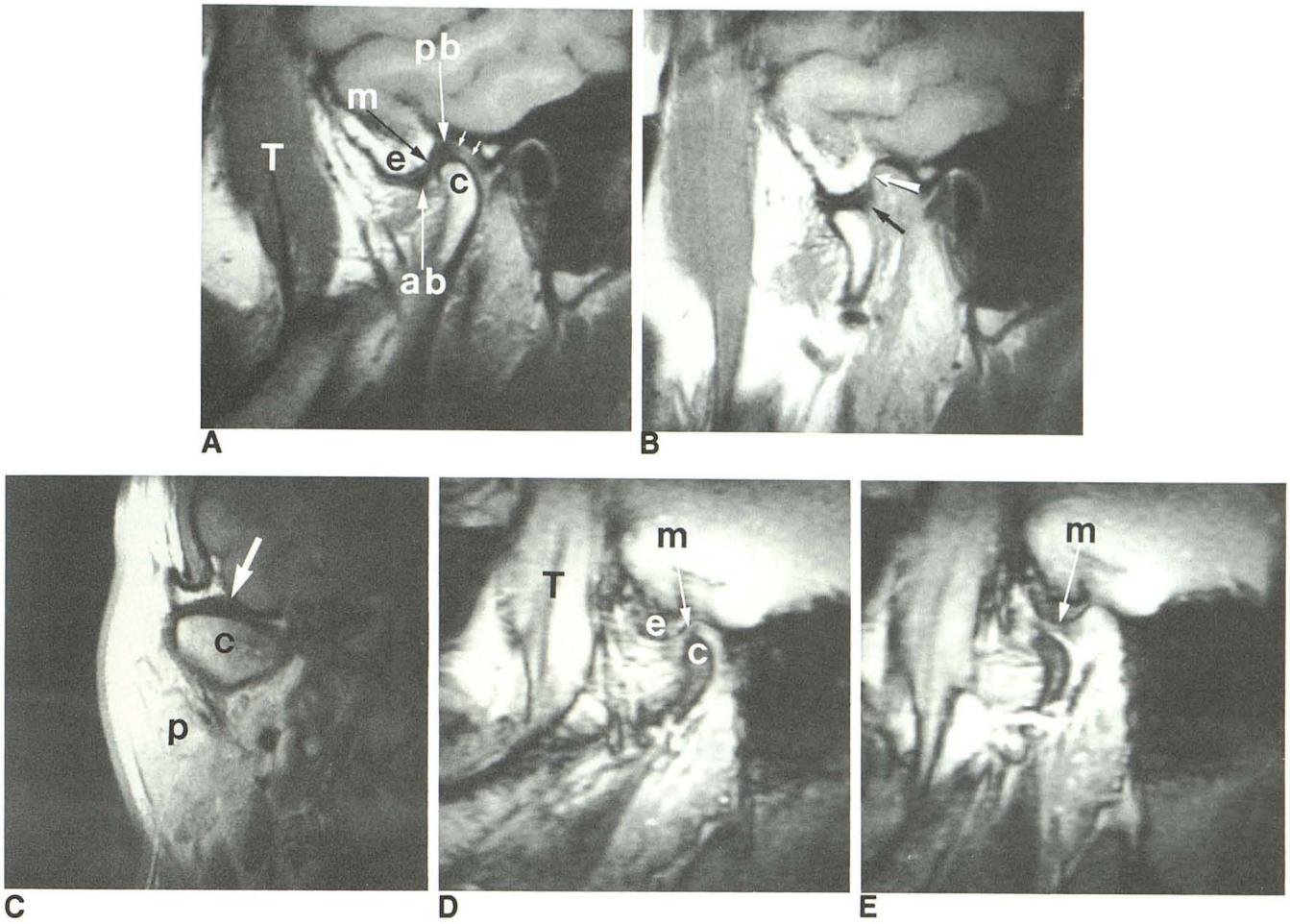

Fig. 2.—Normal temporomandibular joint in closed (*A*) and open (*B*) mouth positions (TR = 500 msec, TE = 20 msec, 256 × 256 matrix, two excitations).

***A*, Meniscus (m) has biconcave appearance and uniform low signal intensity. Posterior band (pb) lies above articular surface of condyle (c). Anterior band (ab) of meniscus lies in front of condyle, proximal to articular eminence (e). Bilaminar zone or posterior meniscus attachment (*arrows*) connects meniscus to temporal bone behind condyle. Temporalis muscle (T) attached onto coronoid process and medial surface of mandible.**

***B*, After translation, condyle lies below eminence. Posterior band of meniscus (*black arrow*) now lies behind condyle. Bilaminar zone (*white arrow*) is redundant owing to limited forward condylar excursion, commonly observed on T1-weighted open-mouth MR images.**

***C*, Coronal image (TR = 500 msec, TE = 20 msec, 256 × 256 matrix, one acquisition) shows normal meniscus (*arrow*) centrally located relative to articular surface of condyle (c). Note adjacent normal parotid gland (p).**

***D* and *E*, Closed (*D*) and open (*E*) mouth partial-flip-angle images (same joint as *A–C*) (TR = 21 msec, TE = 12.5 msec, 30° flip angle, 128 × 256 matrix, two acquisitions, 6-sec image, 5 mm thick).**

***D*, Condyle (c) and eminence (e) exhibit diminished signal intensity (compare with *A*) owing to T2* effects. Meniscus (m) and temporalis muscle (T) are defined less sharply than on T1-weighted images.**

***E*, Maximal open-mouth view shows greater degree of forward condylar movement compared with *B*. Meniscus is well defined.**

the lateral pterygoids and other masticatory muscles may be observed primarily or in association with various internal derangements. Fibrosis and contracture of the superior belly of the lateral pterygoid muscle may accompany chronic anterior and medial displacement of the meniscus, particularly when there is rupture or perforation of an attenuated posterior attachment. This finding is also sometimes observed after meniscectomy, with or without prosthetic meniscus implants (Fig. 9). Videofluoroscopy and dynamic partial-flip-angle techniques demonstrate that muscle atrophy frequently accompanies meniscus degeneration and bony deformity.

Intrinsic Histochemical and Structural Meniscus Alterations

Intrinsic histochemical changes within the deranged or degenerating meniscus may be diagnosed in vivo. Myxoid degeneration of meniscus fibrocartilage may result in increased signal intensity within a diseased meniscus, with or without displacement, identical to pathologic changes observed within the knee (Figs. 3, 4, 8, and 10) [10–14]. High-resolution T1-weighted images are needed to diagnose intrinsic meniscus lesions, as these changes may not be apparent on T2-weighted images, in part owing to decreased spatial resolu-

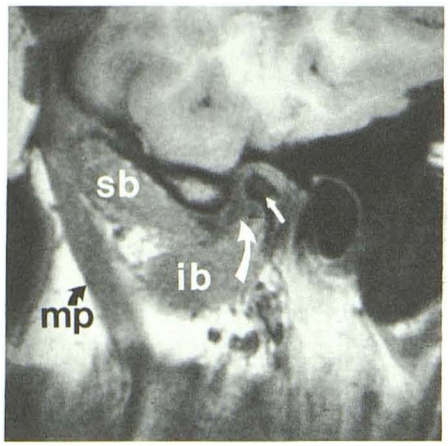

Fig. 3.—Chronic anterior meniscus displacement with normal pterygoid muscles (image through medial pole of condyle), superior belly (sb), and inferior belly (ib) of lateral pterygoid muscle is well defined. Meniscus (*curved arrow*) is anteriorly and medially displaced (medial displacement determined by reviewing sequential lateral to medial images) and shows increased signal (compare with Fig. 2A). Medial pterygoid muscle (mp) lies deep to temporalis muscle. Note diminished signal (*straight arrow*) from hyperostosis in condyle.

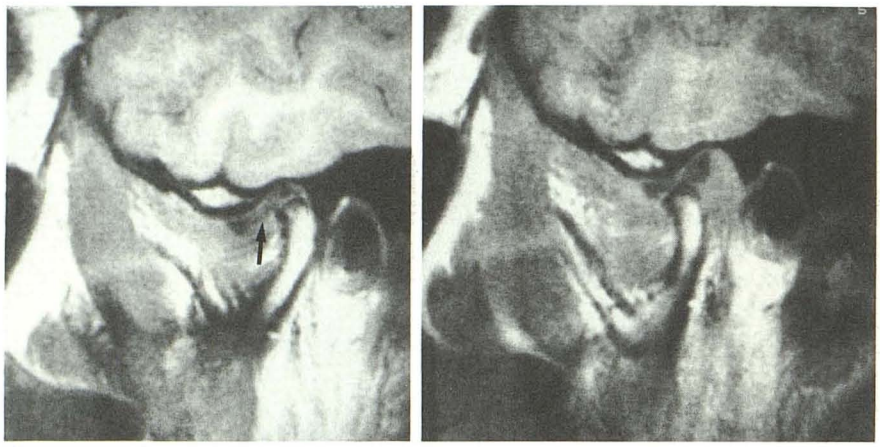

Fig. 4.—Anterior meniscus displacement (*arrow*) with reduction (*B*) in 29-year-old woman with 2-year history of temporomandibular pain and clicking. Note increased meniscus signal (*arrow*).

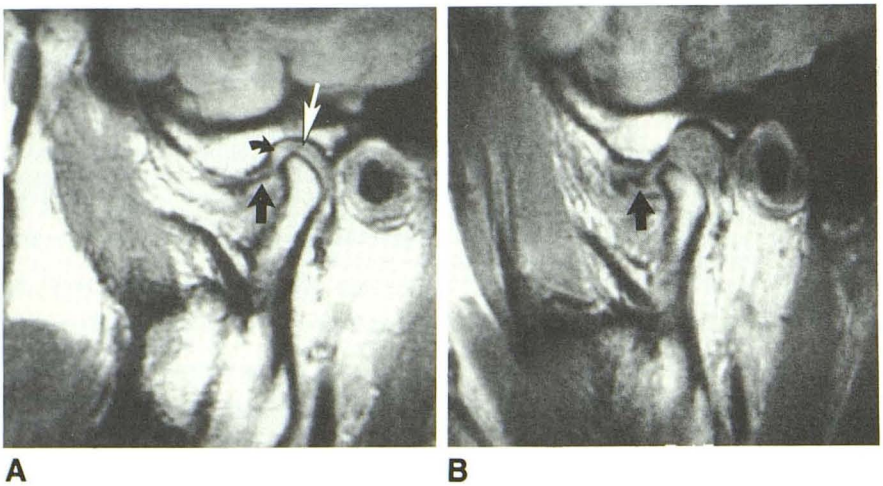

Fig. 5.—Nonreducing chronic meniscus derangement resulting in clinical closed lock.

A, Closed-mouth image shows anterior displacement of meniscus (*straight black arrow*) with stretching of posterior attachment (*white arrow*), which appears attenuated (*curved arrow*) near meniscus attachment (there was no perforation at surgery). Note normal (concentric) condylar positioning within glenoid fossa.

B, Maximal open-mouth view shows nonreduction of thickened and deformed meniscus (*arrow*). Note normal meniscus signal intensity despite chronic displacement and deformity.

tion. With current technology, the normal disk may appear inhomogeneous with 5-mm-thick partial-flip-angle images owing to decreased spatial resolution; therefore, thin-section high-resolution T1-weighted images are recommended for detection of these abnormalities.

Trauma

MR may be used to evaluate the traumatized TMJ for assessment of the severity of injury and surgical planning. Traumatic derangement may result in chronic pain and diminished condylar translation clinically. Muscle spasm, headaches, bony alterations, muscular contracture, and malocclusion are known sequelae of fractures involving the condyle and condylar neck [15]. TMJ hematomas frequently occur with condylar fractures and direct blows to the mandible and commonly result in formation of adhesions (Figs. 11–13). Adhesions are seen as areas of diminished signal intensities on T1-weighted images surrounding or adjacent to the meniscus and condyle, often obliterating the normal fibrofatty tis-

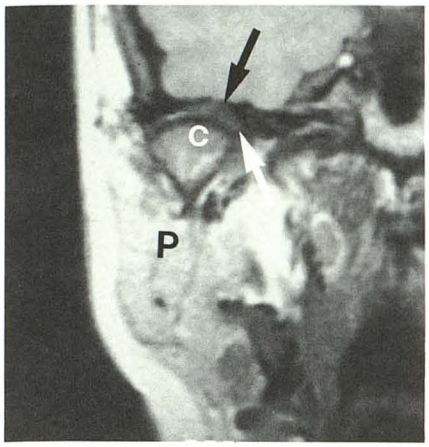

Fig. 6.—Medial displacement of meniscus (3-mm-thick T1-weighted coronal image, obtained with head coil). Posterior band of meniscus (*arrows*) is medially displaced on top of condyle (c). Parotid gland (P) appears normal. Abnormality was detected during head examination performed to evaluate ipsilateral headache and facial pain.

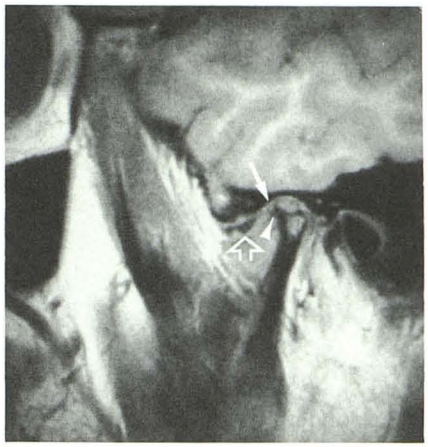

Fig. 7.—Late-stage internal derangement with perforation (surgically proved) of posterior attachment. Meniscus (*open arrow*) is displaced and deformed. Condyle is deformed, and there is an anterior osteophyte (*arrowhead*). Bilaminar zone is attenuated in area of perforation (*solid arrow*).

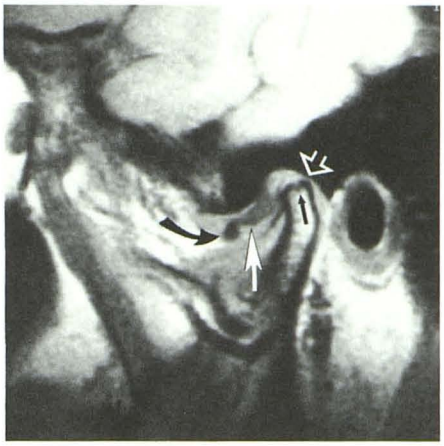

Fig. 8.—Chronic anterior meniscus displacement (*white arrow*) with increased signal and perforation (surgically proved) of posterior attachment. Anterior attachment (*curved arrow*) is redundant and thickened. Condyle is posteriorly displaced within glenoid fossa and contacts temporal bone posteriorly (*open arrow*) at point of perforation. Small focus of avascular necrosis (*straight black arrow*) is seen in articular surface of condyle.

Fig. 9.—Atrophy and fibrosis of superior belly (*arrows*) of lateral pterygoid muscle after meniscectomy and permanent implant placement. Inferior belly (ib) is normal.

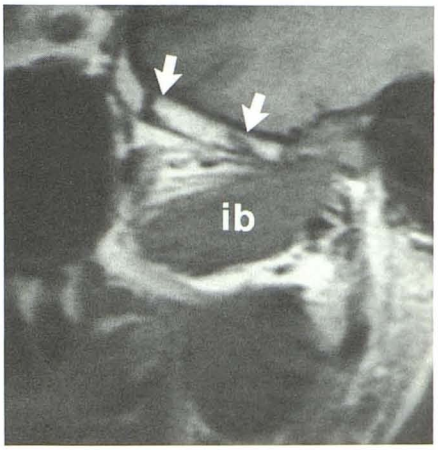

9

Fig. 10.—Increased signal intensity (*straight arrows*) within normally positioned meniscus (*curved arrow*). Note unusually deep glenoid fossa. Clinical symptoms included long-standing headache, facial pain, temporomandibular joint clicking, and episodic locking.

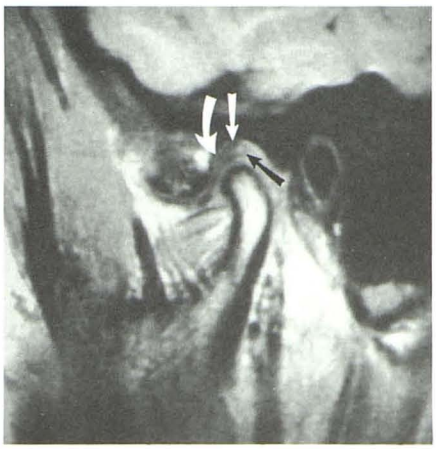

10

sues seen in normal joints [2, 5, 11]. MR is of particular value in the evaluation of late, traumatic sequelae, since soft-tissue structural alterations often cannot be seen with conventional imaging techniques, and arthrography/videofluoroscopy may be difficult to perform when adhesions are present.

Postoperative TMJ

A number of surgical procedures have been described for the correction of internal derangements [15–22]. Simple meniscectomy and meniscus plication procedures are all commonly performed surgical procedures. Condylectomy and reduction osteotomy of the articular eminence (eminectomy) are used less often. A number of different temporary and permanent meniscus implants after disk removal have been and continue to be used. MR permits direct evaluation of the postoperative joint. Limited skull films and conventional lateral tomograms are helpful in conjunction with MR, as it is important to distinguish calcification from hypointense scar tissue. This combination generally clarifies the type and extent of prior joint manipulation. Submentovertex and posteroanterior

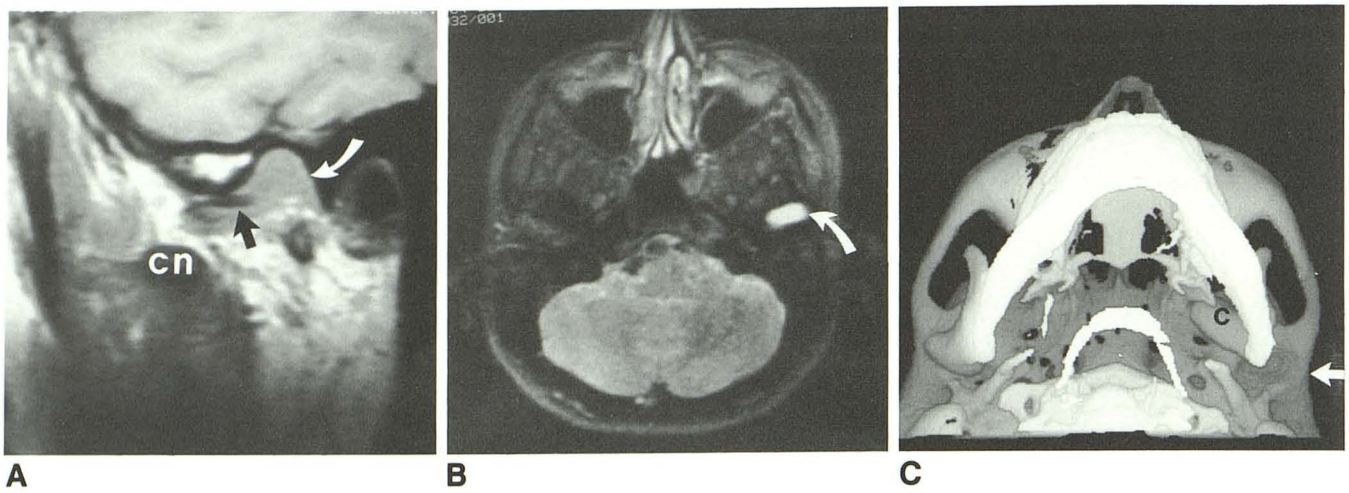

Fig. 11.—Subacute temporomandibular joint trauma.

A, Sagittal closed-mouth image (256 × 128 matrix) shows rotational dislocation of condyle out of glenoid fossa (*white arrow*) owing to condylar neck (cn) fracture. Meniscus (*black arrow*) is anteriorly and medially displaced by lateral pterygoid contracture.

B, Axial spin-echo (TR = 2000 msec, TE = 80 msec) image, 5 mm thick, shows fluid (*arrow*) filling glenoid fossa.

C, 3-D CT scan shows anteromedial displacement of condyle (c) owing to condylar neck fracture. Glenoid fossa (*arrow*) is empty. At surgery, performed to reduce complete closed lock and reposition condyle, adhesions, fluid, and blood breakdown products were found within glenoid fossa above displaced meniscus.

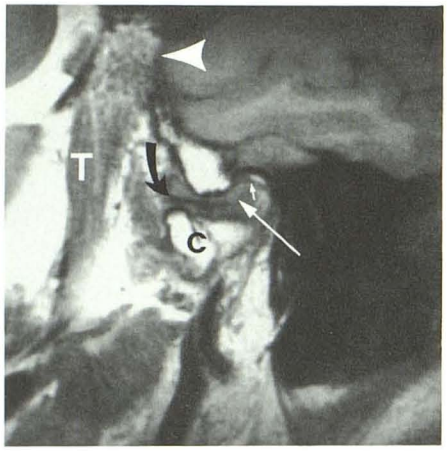

Fig. 12.—Chronic deformity from old intracapsular fracture of condyle (c). Meniscus (*curved arrow*) exhibits normal signal intensity and is normally positioned relative to deformed condyle. Posterior attachment (*short white arrow*) is redundant and separated from meniscus because of large perforation (*long white arrow*) encountered at surgery. Note scarring and fibrosis within medioposterior aspect of temporalis muscle (T) insertion (*arrowhead*).

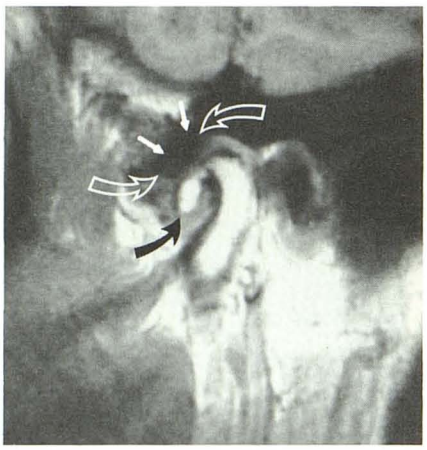

Fig. 13.—Chronic adhesions and dystrophic ossification (*black arrow*) secondary to old trauma. Meniscus (*open arrows*) was found to be totally adherent to temporal bone (*straight arrows*) due to extensive adhesions. Soft-tissue calcification was present throughout joint space.

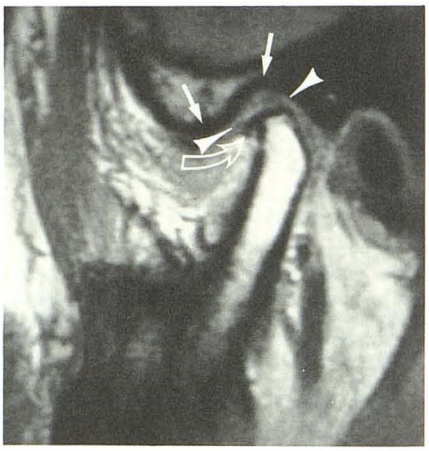

Fig. 14.—Optimal 12-month postmeniscectomy temporomandibular joint. Articular cortex of temporal bone (*straight arrows*) is slightly thickened but retains its normal sigmoid curvature. Articular space (*arrowheads*) is maintained by articular-bearing surface cartilage and fibrofatty tissue on this closed-mouth image. Note prominent attachment from inferior belly of lateral pterygoid muscle (*curved arrow*), shown to be noncalcified on conventional lateral temporomandibular joint tomograms.

open-mouth, jaw-protruded views of the mandible are also helpful, since discrepancies in condylar shape and height may be detected as degenerative remodeling consequences of chronic internal derangements, trauma, and surgical manipulation of the joint.

After meniscectomy, the amputated posterior and anterior meniscal attachments are seen at the margins of the articular space (Figs. 14 and 15). Typically, some remodeling changes result in thickening of the articular surfaces of both the glenoid fossa and condyle, both of which may become slightly flattened. Ideally, the articular space is maintained by bearing surface fibrocartilage. Temporary meniscus implants are commonly used after meniscectomy to prevent the formation of adhesions. Postoperative bony remodeling changes may be

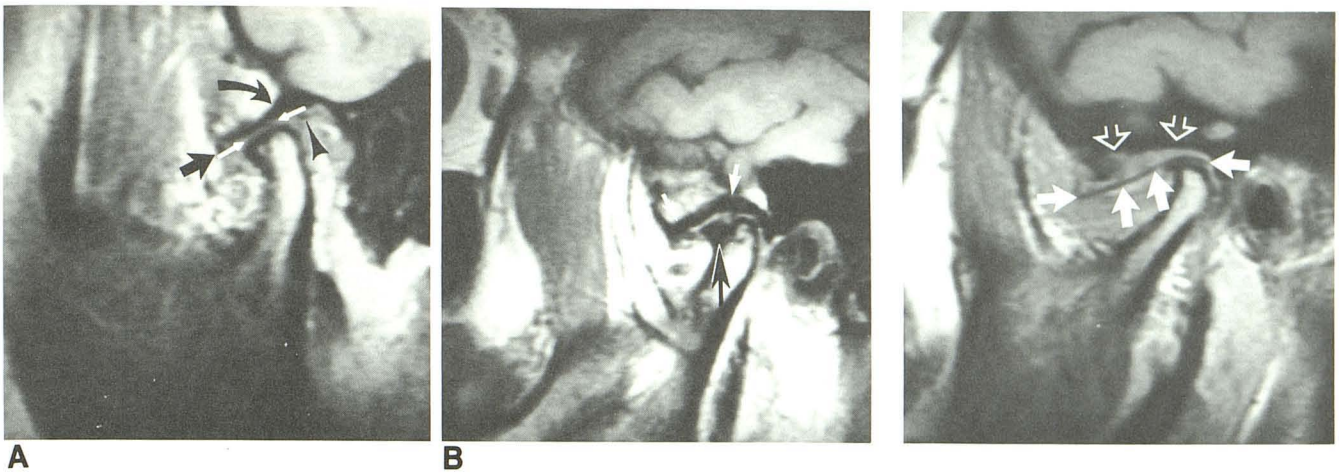

Fig. 15.—Postoperative changes after simple meniscectomy (*A*) and multiple operations including initial permanent prosthesis implantation (*B*).

A, Closed-mouth image shows amputated anterior (*straight black arrow*) and posterior (*arrowhead*) meniscal attachments 42 months after surgery. Joint space (*white arrows*) is present and articular surfaces of condyle and temporal bone (*curved arrow*) are flattened owing to remodeling.

B, Advanced degenerative change 18 months after meniscectomy and permanent implant insertion that subsequently required removal because of joint pain and swelling. Cortex of temporal bone (*white arrows*) is thickened and irregular. Large condylar osteophyte (*black arrow*) is seen anteriorly. Surgery was performed again after imaging for lysis of adhesions.

Fig. 16.—Permanent meniscus implant (Proplast) 6 months after insertion. Hypointense prosthesis (*solid arrows*) is sharply demarcated from adjacent tissues. Note postsurgical changes in temporal bone (*open arrows*), where implant is anchored.

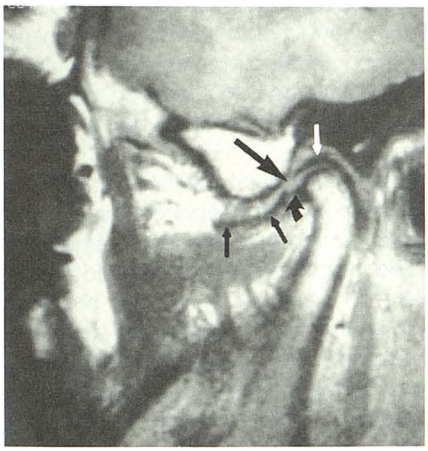

Fig. 17.—Perforation (*long straight arrow*) of permanent Silastic implant (*short straight arrows*) 42 months after insertion. Anterior condylar osteophyte (*curved arrow*) lies beneath perforation. Note absence of destructive skeletal changes with this implant.

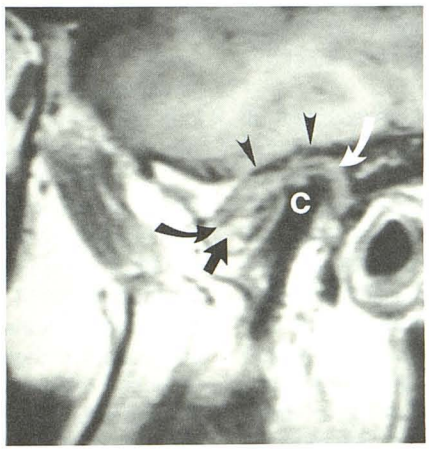

Fig. 18.—Destructive changes associated with permanent meniscus implant (18 months after meniscectomy and Proplast prosthesis insertion). Marked irregularity of condyle (c) is noted with decreased signal intensity interpreted to represent avascular necrosis. Prosthesis (*curved arrows*) is surrounded by highly vascular granulation tissue (*straight arrow*), removed along with prosthesis. Marked irregularity of temporal bone (*arrowheads*) is noted.

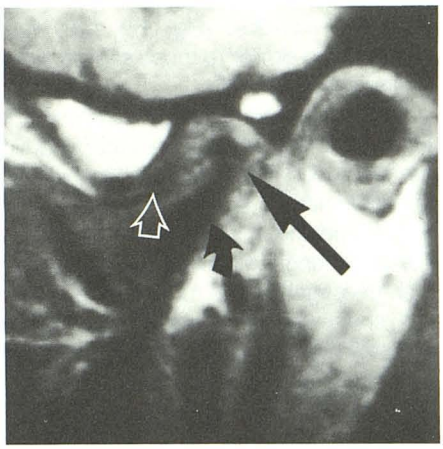

Fig. 19.—Old avascular necrosis and condylar deformity in 31-year-old man with history of bilateral sagittal split mandibular osteotomies and orthognathic manipulation at 25 years of age. Condyle (*straight solid arrow*) and condylar neck (*curved arrow*) are deformed and lack normal signal intensity. Note displaced meniscus (*open arrow*) and condylar malposition within glenoid fossa. (Changes were bilateral.)

distinguished from ordinary osteoarthritis by using conventional tomography alone; however, MR is needed to observe adhesions and other soft-tissue structures within the joint [5, 10, 11]. Relative narrowing of the articular space is often observed without functional disturbance after successful meniscectomy (Fig. 15A). Irregular articular surfaces and adhesions can result from unsuccessful surgery with permanent meniscus implants (Fig. 15B). In this circumstance, the patient may experience pain, crepitus, and limitation of joint motion.

Permanent meniscus prostheses are easily studied with MR (Figs. 16–18). Granulation tissue, joint fluid, and adhesions may be detected. Perforation of an implant can occur (Fig. 17). Destructive changes observed with certain perma-

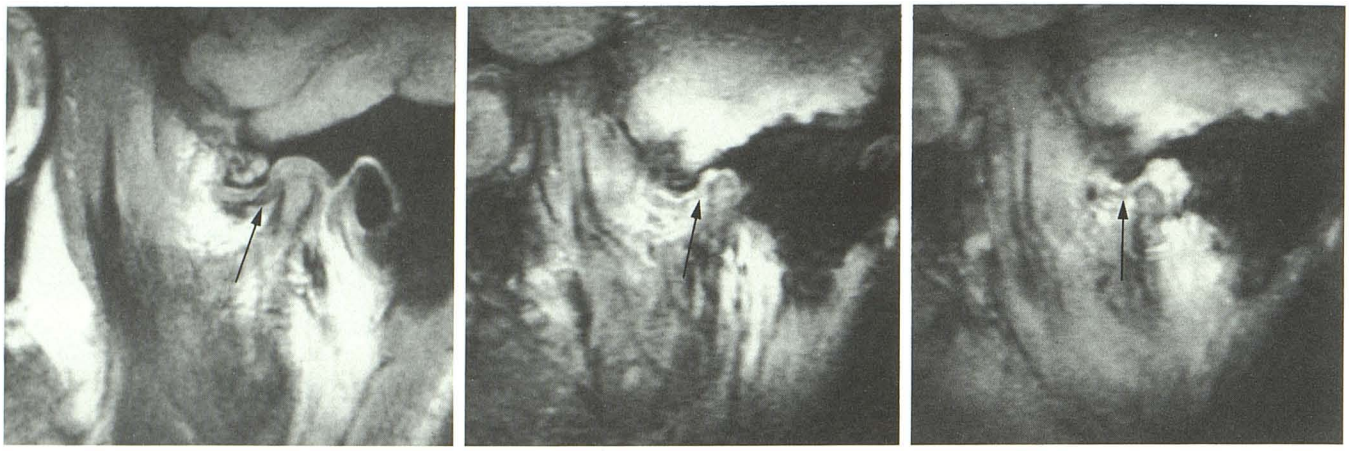

Fig. 20.—Standard T1-weighted (*A*) and 3-sec, partial-flip-angle (*B* and *C*) images show nonreducing meniscus derangement.
***A*, Meniscus (*arrow*) is displaced and deformed.**
***B* and *C*, Closed- (*B*) and maximal open- (*C*) mouth GRASS images (TR = 21 msec, TE = 12.5 msec, 30° flip angle, 256 × 128 matrix, one acquisition, 3 sec) show nonreduction of displaced meniscus (*arrows*).**

nent implants may be assessed, along with physiologic alterations in bony structures (Fig. 18) [23]. Avascular necrosis of the condyle and consequent remodeling changes may follow jaw trauma or orthognathic and surgical manipulation of the TMJ and mandible (Fig. 19). MR signal and morphologic changes are similar to those seen in avascular necrosis of the femoral head [24–26].

Partial-flip-angle imaging techniques permit assessment of joint physiology when sequential dynamic imaging techniques are employed. With GRASS techniques, any number of sequential images can be obtained at incremental degrees of mouth opening in as little time as 3 sec per image (Fig. 20). Partial-flip-angle techniques show immense promise for further investigation into functional derangements of the meniscus and muscles of mastication. Videofluoroscopy of the injected TMJ provides higher spatial resolution of the meniscus; however, this procedure is invasive; requires considerable technique, skill, and expertise on the part of the arthrographer; and does not allow direct observation of jaw musculature.

MR has limitations. Claustrophobia precludes MR imaging of certain patients, while some apprehensive patients may be examined successfully after sedation. Older ferromagnetic dental appliances may cause image degradation, which may on occasion result in inadequate image quality for interpretation. Patient motion may significantly degrade image quality; however, this problem is minimized when patients are properly positioned and secured relative to the surface coil and reminded frequently during the procedure not to move. Partial-flip-angle techniques dramatically reduce image acquisition times and diminish many of the problems related to patient motion, although spatial resolution is sacrificed. With the advent of routine nonorthogonal imaging capability and thin-section three-dimensional volume acquisitions, problems of partial-volume averaging caused by unusual joint orientation will be diminished. Limited skull films including submentovertex and open-mouth, jaw-protruded anteroposterior projections of the skull base and mandible provide useful and important information regarding condylar symmetry and orientation. These data are used during positioning of the patient for an MR examination. When limited skull films and high-quality closed- and open-mouth lateral tomograms are combined with surface-coil MR, patients with advanced meniscus derangements can be evaluated satisfactorily with closed-mouth MR images alone.

We believe that a symptomatic joint exhibiting meniscus displacement, deformity, and intrinsic degeneration is best treated with meniscectomy. In advanced cases, a temporary Silastic implant is inserted into the joint and removed percutaneously after 4 weeks. The temporary implant prevents formation of adhesions in the joint recesses in the early postoperative days. The presence or absence of meniscus reduction relative to the condyle is less important when deformity and intrinsic alterations accompany anterior displacement. Such changes are irreversible and often progress to perforation and subsequent development of osteoarthritis. Meniscectomy performed before perforation both relieves bothersome mechanical symptoms and decreases the likelihood that osteoarthritis will develop.

ACKNOWLEDGMENT

We thank Steven D. Johnson for recent surgical confirmation of the findings in Figure 17.

REFERENCES

1. Katzberg RW, Schenck JF, Roberts D, et al. Magnetic resonance imaging of the temporomandibular joint meniscus. *Oral Surg* **1985**;59:332–335
2. Harms SE, Wilk RM, Wolford LM, et al. The temporomandibular joint: magnetic resonance imaging using surface coils. *Radiology* **1985**;157:133–136
3. Katzberg RW, Bessette RW, Tallents RH, et al. Normal and abnormal

temporomandibular joint: MR imaging with surface coil. *Radiology* **1986**;158:183–189
4. Schellhas KP, Wilkes CH, Heithoff KB, Omlie MR, Block JC. Temporomandibular joint: diagnosis of internal derangements using magnetic resonance imaging. *Minn Med* **1986**;69:516–519
5. Harms SE, Wilk RM. Magnetic resonance imaging of the temporomandibular joint. *Radiographics* **1987**;7(4):521–542
6. Wilkes CH. Arthrography of the temporomandibular joint in patients with the TMJ-pain-dysfunction syndrome. *Minn Med* **1978**;61:645–652
7. Christensen EL, Thompson JR, Hasso AN, Hinshaw DB. Correlative thin section temporomandibular joint anatomy and computed tomography. *Radiographics* **1986**;6(4):703–723
8. Westesson TL. Diagnostic accuracy of double contrast arthrotomography of the temporomandibular joint: correlation with postmortem morphology. *AJNR* **1984**;5:463–468
9. Mills TC, Ortendahl DA, Hylton NM, Crooks LE, Carlson JW, Kaufman L. Partial flip angle MR imaging. *Radiology* **1987**;162:531–539
10. DeBont LGM, Boering G, Liem RSB, et al. Osteoarthritis and internal derangement of the temporomandibular joint: a light microscopic study. *J Oral Maxillofac Surg* **1986**;44:634–643
11. DeBont LGM. Temporomandibular joint articular cartilage structure and function [Doctoral Thesis]. Groningen, The Netherlands: University of Groningen, **1985**
12. Reicher MA, Bassett LW, Gold RH. High-resolution magnetic resonance imaging of the knee joint: pathologic correlations. *AJR* **1985**;145:903–909
13. Reicher MA, Flartzman S, Duckwiler GR, et al. MR imaging of the knee. *Radiology* **1987**;162:547–551
14. Stoller DW, Martin C, Crues JV III, Kaplan L, Mink JH. Meniscal tears: pathological correlation with MR imaging. *Radiology* **1987**;163:731–735
15. Norman JE. Post-traumatic disorders of the jaw joint. *Ann R Coll Surg Engl* **1982**;64:27–36
16. Gallagher DM, Wolford LM. Comparison of Silastic and proplast implants in the temporomandibular joint after condylectomy for osteoarthritis. *J Oral Maxillofac Surg* **1982**;40:627–630
17. Marciani RD, Ziegler RC. Temporomandibular joint surgery: a review of 51 operations. *Oral Surg* **1983**;56:472–476
18. Hall MB. Meniscoplasty of the displaced temporomandibular joint meniscus without violating the inferior joint space. *J Oral Maxillofac Surg* **1984**;42:788–792
19. Oaitis GW Jr, Baker DA. The bilateral eminectomy as definitive treatment. A review of 44 patients. *Int J Oral Surg* **1984**;13:294–298
20. Eriksson L, Westesson PL. Long-term evaluation of meniscectomy of the temporomandibular joint. *J Oral Maxillofac Surg* **1985**;43:263–269
21. Bessette RW, Katzberg RW, Natiella JR, Rose MJ. Diagnosis and reconstruction of the human temporomandibular joint after trauma or internal derangement. *Plast Reconstr Surg* **1985**;75:192–205
22. Sawhney CP. Bony ankylosis of the temporomandibular joint: follow-up of 70 patients treated with arthroplasty and acrylic spacer interposition. *Plast Reconstr Surg* **1986**;77:1–6
23. Lagrotteria L, Scapino R, Granston AS, Felgenhauer D. Patient with lymphadenopathy following temporomandibular joint arthroplasty with proplast. *J Craniomand Pract* **1986**;4(2):172–178
24. Dooms GC, Fisher MR, Hricak H, Richardson M, Crooks LE, Genant HK. Bone marrow imaging: magnetic resonance studies related to age and sex. *Radiology* **1985**;15:429–432
25. Thickman D, Axel L, Kressel HY, et al. Magnetic resonance imaging of avascular necrosis of the femoral head. *Skeletal Radiol* **1986**;15:133–140
26. Markisz JA, Knowles JR, Altchek DW, et al. Segmental patterns of avascular necrosis of the femoral heads: early detection with MR imaging. *Radiology* **1987**;162:717–720